



ELSEVIER

Journal of Crystal Growth 142 (1994) 156–164

JOURNAL OF  
**CRYSTAL  
GROWTH**

# Crystal–protein interactions studied by overgrowth of calcite on biogenic skeletal elements

J. Aizenberg, S. Albeck, S. Weiner, L. Addadi \*

*Department of Structural Biology, Weizmann Institute of Science, Rehovot 76100, Israel*

Received 5 May 1994

## Abstract

A key parameter in the biological control of crystal formation is the interaction of a group of acidic macromolecules with the mineral phase. Here we study protein–calcite interactions using epitaxial overgrowth of synthetic calcite crystals under conditions in which local release of occluded macromolecules from the biogenic substrate occurs. The macromolecules subsequently interact with the newly formed overgrown crystals, resulting in modified calcite morphology. This novel method provides a means of mapping crystal–protein interactions under conditions that minimally affect the conformational states of the acidic macromolecules. We show that proteins released from calcitic sponge spicules and mollusc prisms specifically interact with {001} and {011} faces of calcite, whereas proteins released from echinoderm skeletal elements only interact with {011} faces. The extent to which the overgrown crystals are affected by the proteins varies even in the same organism and within the same element, depending on the site and crystallographic orientation of the skeletal elements.

## 1. Introduction

Minerals are used by many different organisms for a wide variety of functions [1,2]. Despite the enormous diversity of this phenomenon, it has been observed that in almost every case in which control is exerted over the mineralization process, a group of acidic macromolecules are present [2]. These proteins and glycoproteins are both associated with the crystal surfaces, and are found within the biogenic crystals themselves. They are generally thought to be involved in controlling the skeleton formation processes [3–5].

Proteins from within calcitic biogenic phases were shown to interact in vitro from solution with growing calcite crystals [6]. Once adsorbed on the surface, they are overgrown and are consequently occluded within the crystal itself. The resulting morphology of the synthetic crystals is an expression of different growth rates in the various crystallographic directions, modulated by the adsorbed additives present in solution. The rule is normally that the planes on which the additives are adsorbed become expressed as stable crystal faces [7]. The morphological changes that occur in calcite crystals grown from solutions containing acidic macromolecules from the sea urchin skeleton show that they interact preferentially with a family of crystal faces of the type {011}, which are approximately parallel to the crystallographic  $c$ -

\* Corresponding author.

axis [8]. In contrast, the main protein fraction isolated from the single prisms of mollusc shells is intercalated on the (001) planes [8]. Synchrotron X-ray studies of a variety of biologically formed calcite single crystals demonstrate that their textural properties, namely size and alignment of the crystallographically perfect domains, are also under biological control [9]. Sea urchin spines and mollusc prisms show textural anisotropy consistent with intercalation of additives on planes parallel to and perpendicular to the *c*-axis, respectively, in agreement with the morphological modification data. We thus suggested that the control of textural properties is exerted, at least in part, by the occlusion of the acidic macromolecules.

A key to understanding the mechanisms and functions of the biogenic single crystal–protein composites is the recognition process between the macromolecule and the crystal face. Here we use a new crystal overgrowth technique for studying specific crystal–macromolecule interactions. We have adapted a fairly simple procedure used for mapping crystallographic axes orientations in biogenic elements that do not express crystal faces [10–12]. The technique involves epitaxial overgrowth of new calcite crystals on the single crystalline skeletal elements. The orientation and morphology of the newly-formed calcite rhombohedra unequivocally define their crystal axes directions, and thereby the crystallography of the substrate as well. By slowing down the rate at which calcite crystals grow epitaxially on the biogenic substrate, we were surprised to observe crystal faces other than those of the stable cleavage {104} habit. These faces develop as a result of selective readsorption of the macromolecules released from the biogenic element. We were thus able to obtain information on specific crystal–protein interactions localized in different areas of the skeleton, and under conditions which probably preserve the intracrystalline proteins close to their native state.

## 2. Experimental procedure

*Collection and preparation of the material.* Specimens of the calcareous sponge *Clathrina coriacea* (eastern Mediterranean) were collected

and maintained alive in sea water. They were then washed with fresh water and frozen in liquid nitrogen to prevent further crystallization or dissolution of calcium carbonate. Immediately after thawing, the spicules were extracted and cleaned by immersion in 2.5% NaOCl solution on a rocking table for 1 h. Sodium hypochlorite was removed by centrifugation and the liberated spicules were washed several times in double-distilled water (DDW) and dried immediately.

Shells of the bivalve mollusc *Atrina serrata* (North Carolina) were collected fresh, cleaned and stored dry. The calcitic prismatic layer was mechanically separated from the inner nacreous layer and treated with concentrated NaOCl solution followed by constant stirring for 4 days. The crystal suspension was sonicated, then extensively washed with DDW and separated by decantation.

Fresh specimens of the sea urchin *Paracentrotus lividus* (eastern Mediterranean) and the brittle star *Ophiocoma wendti* (Florida) were stored at room temperature after drying. Individual spines and ossicles were cleaned by hypochlorite treatment for 1 day, as described above for sponge spicules.

Single crystalline skeletal elements were initially examined in a JEOL 6400 scanning electron microscope (SEM), to verify surface cleanliness and to check that no etching had occurred. Magnesium contents were determined by atomic absorption.

*The epitaxial overgrowth of calcite crystals* on very small biogenic substrates (the mollusc prisms and sponge spicules) was achieved by drying a drop of a suspension of the skeletal elements in water on a clean glass cover slip (1.3 cm diameter). The coverslips were then placed in a Nunc multidish used for cell culture (well diameters 1.5 cm). The larger skeletal elements (echinoderm spines and ossicles) were placed directly in the wells in different orientations, as overgrowth is not uniform on all surfaces. The specimens were overlaid with 1.5 ml of 7.5mM calcium chloride solution. Calcite crystals were grown for 3 days in a closed desiccator which contained vials of ammonium carbonate powder. The overgrown specimens (whole cover slips or the larger elements themselves) were then lightly rinsed in DDW,

dried and examined in the SEM after coating with gold. Rapid calcite overgrowth from a mixture of 0.1M calcium chloride and 0.1M sodium carbonate solutions [12] was performed for comparison.

*Extraction of intracrystalline macromolecules* was performed by decalcification in 0.5M ethylenediamine tetra-acetic acid (EDTA). The solution was then dialysed (Spectrapor 3 dialysis tubing), centrifuged at 10,000 g, and lyophilized to

reduce the volume if necessary. Amino acid analysis (Dionex BIOLC) was used for obtaining protein concentrations.

*Crystal growth experiments.* Synthetic calcite crystals were grown in the presence of 1.0  $\mu\text{g}/\text{ml}$  of the total sponge spicule soluble proteins or 2.0  $\mu\text{g}/\text{ml}$  of sea urchin spine proteins. Calcite crystals grown in the absence of any additives and those formed in the presence of traces of EDTA only, were used as controls.

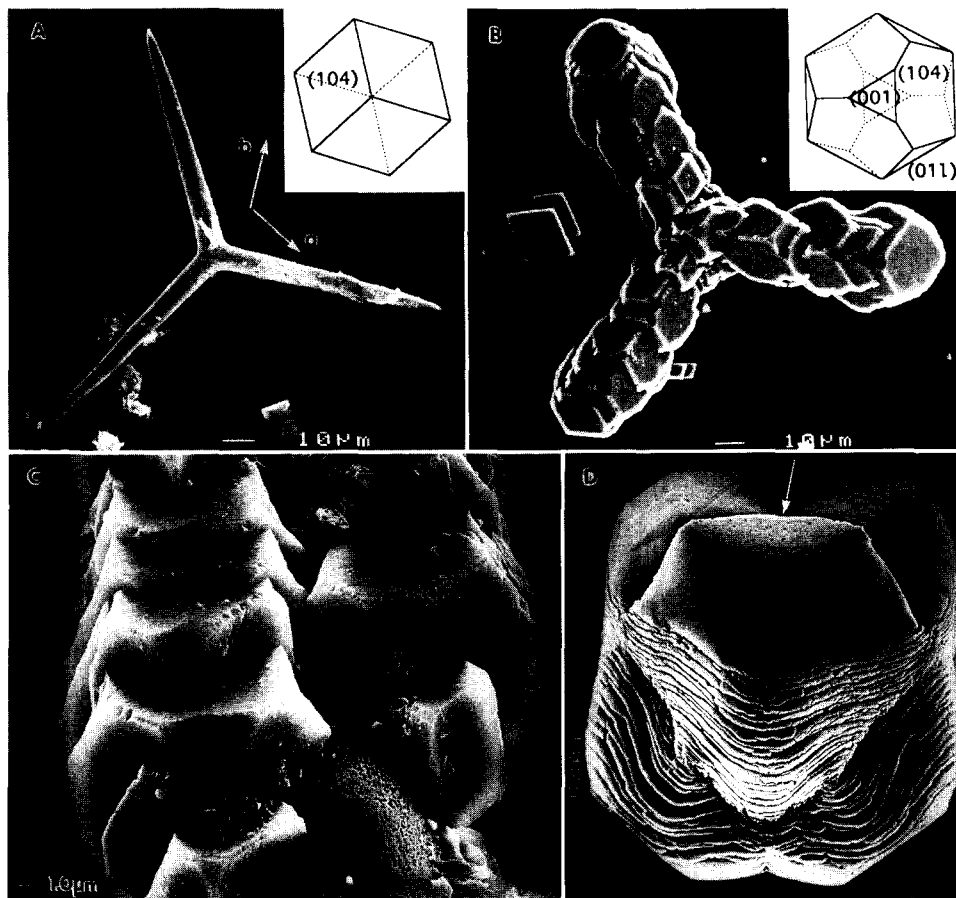


Fig. 1. (A) Triradiate spicule from the sponge *Clathrina coriacea* after NaOCl treatment. The directions of the crystallographic  $a$ -axes are indicated. The  $c$ -axis is perpendicular to the plane of the spicule. Insert: computer simulation of a pure synthetic calcite crystal, viewed in the same orientation as the spicule. The computer simulation is based on the crystallographic parameters of calcite. (B) Triradiate spicule after slow overgrowth. Note the development of the {001} and {011} faces on the overgrown crystals, and their absence in the isolated crystals. Insert: computer simulation of the morphology of the overgrown crystals with the same developed habit. (C) Enlargement of one overgrown spicule ray, showing the etched original surface, as well as the overgrown crystals with the newly developed faces. (D) Synthetic calcite crystal grown in the presence of EDTA extracted total sponge spicule proteins (1.0  $\mu\text{g}/\text{ml}$ ). The well-developed {001} face is indicated by the arrow. The use of EDTA results in the formation of the stepped surface parallel to the  $c$ -axis.

Identification of newly formed faces was achieved by viewing calcite crystals with their  $\{01\}$  and corresponding  $\{104\}$  faces both edge-on in the SEM. In this position the crystallographic  $c$ -axis lies in the plane of the picture, forming a  $45^\circ$  angle with the  $\{104\}$  face. The index  $l$  was determined by measuring the angle  $\Delta$  between the  $c$ -axis and the unknown  $\{01l\}$  plane using the equation

$$l = (c \tan \Delta) / (a \cos 30^\circ),$$

where  $a$  and  $c$  are calcite cell dimensions (see Fig. 3B, insert). This procedure makes possible the morphological analysis of these very small

crystals which cannot be measured by X-ray diffraction.

### 3. Results

Fig. 1A shows a SEM micrograph of a calcitic spicule from the sponge *Clathrina coriacea*. This triradiate spicule is reported to be a single crystal [13]. Its morphology reflects the hexagonal symmetry of calcite. The  $c$ -axis is oriented perpendicular to the plane of the spicule, and the  $a^*$ -axes are along the rays. The surface of the element is rounded, very smooth, and expresses none of the

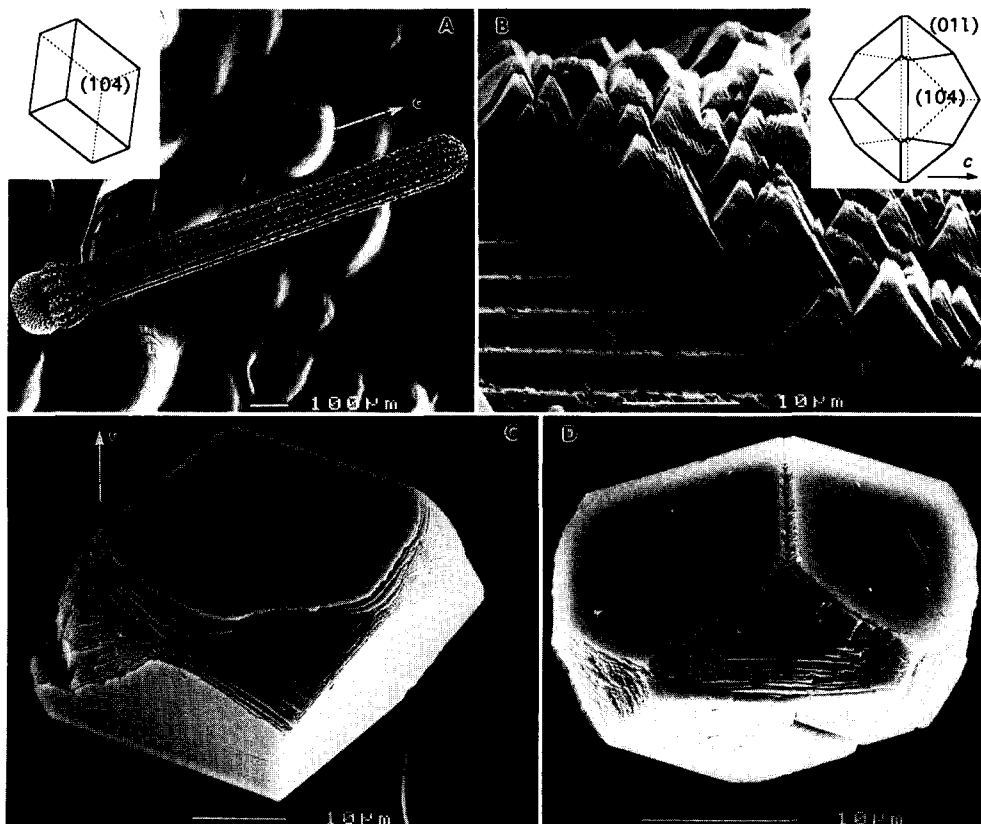


Fig. 2. (A) *Paracentrotus lividus* spine. The direction of the  $c$ -axis is indicated. Insert: computer simulation of a pure synthetic calcite crystal, viewed in the same orientation as the spine. (B) Enlargement of part of an overgrown spine, showing the etched original surface and the newly formed crystals. Note the development of faces roughly parallel to the  $c$ -axis. Insert: computer simulation of the morphology of the overgrown crystals. (C) Enlargement of one overgrown crystal with well-developed  $\{01l\}$  and  $\{104\}$  faces, as shown in the insert in (B). The direction of the  $c$ -axis is indicated. (D) Synthetic calcite crystal grown in the presence of partially purified protein extract from *P. lividus* spines ( $2 \mu\text{g/ml}$ ).

stable calcite crystallographic faces. In contrast, synthetic crystals grown in the absence of additives always form perfect rhombohedra that exhibit only the stable  $\{104\}$  hexagonal faces. Fig. 1B shows a spicule overgrown under conditions of slow diffusion. Epitaxially formed calcite crystals are all oriented in the same direction, consistent with the known symmetry of the substrate. Moreover, the overgrown crystals exhibit two additional groups of faces other than the  $\{104\}$  set, while those formed from the bulk solution and not in contact with the biogenic material express only the normal rhombohedral habit (Fig. 1B). Measurements of the overgrown crystal faces show that the average angles between the newly formed faces and the  $c$ -axis are  $16^\circ \pm 3^\circ$  and  $89^\circ \pm 1^\circ$ . This implies that the developed faces are approximately parallel to the  $\{01\bar{l}\}$  ( $l = 1\text{--}1.5$ ) and  $\{001\}$  calcite crystallographic planes. Closer examination of the spicule surface shows that it was etched during the overgrowth (Fig. 1C). On the other hand, rapid overgrowth from a mixture of calcium chloride and sodium carbonate solutions causes formation of tiny ( $2\text{--}5\text{ }\mu\text{m}$ ) calcite crystals of regular  $\{104\}$  habit, and the spicule surface is not etched. The observation of new sets of faces on the crystals formed by slow overgrowth raises the possibility that proteins released from the spicule interact specifically with

the growing crystals in the two observed directions.

To examine this possibility, calcite crystals were grown de novo from a saturated solution containing the total assemblage of macromolecules extracted from within the sponge spicules. The crystals obtained do exhibit well-developed smooth  $\{001\}$  faces, are also affected in the  $a$  and  $b$  directions, and show remnants of the  $\{104\}$  habit as well (Fig. 1D). It thus appears that the specific changes in the morphology of the overgrown crystals, most notably the development of the  $\{001\}$  face, can be accounted for by preferential adsorption of macromolecules originally occluded within the sponge spicules. It should be noted, that traces of EDTA remaining in the protein solution after dialysis cause non-specific inhibition of growth with development of faces parallel to the  $c$ -axis [8]. This may prevent the observation of specific macromolecule–crystal interactions on planes parallel to the  $c$ -axis (Fig. 1D).

To further verify that the effect observed during the overgrowth is indeed due to macromolecules released from within the skeletal element, analogous experiments were performed with the better studied echinoid skeleton. Sea urchin spines have a complex and convoluted ultrastructure (Fig. 2A). The entire spine is composed of a single calcite crystal [14], despite its

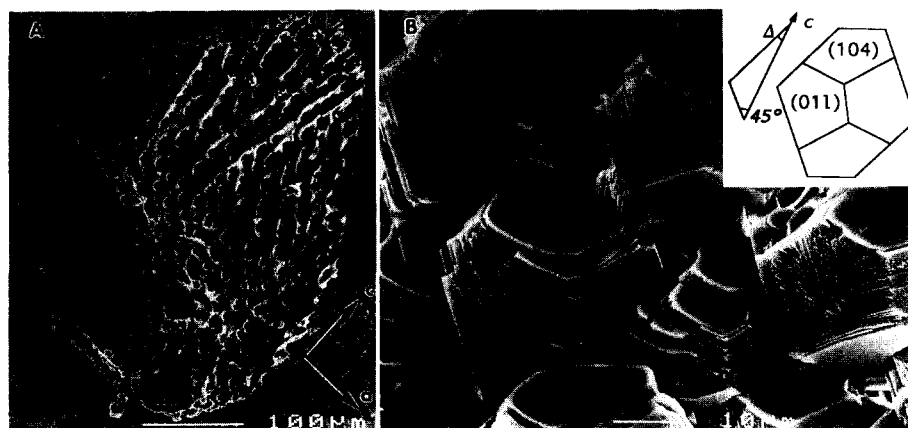


Fig. 3. (A) Tentacle scale from the brittle star *Ophiocoma wendti*. The directions of the  $a$ - and  $c$ -axes are indicated. (B) Area of an overgrown tentacle scale, showing the strongly affected newly formed crystals. Insert: computer simulation of the morphology of the overgrown crystals with well-developed  $\{01\bar{l}\}$  faces, oriented in the same direction as the ossicle. One affected and one  $\{104\}$  face are edge-on, in the geometry that is used for identification of the newly formed faces (see text).

smooth and rounded surfaces. Upon overgrowth, the element also undergoes slight etching (Fig. 2B). The overgrown crystals are all perfectly aligned with their  $c$ -axes parallel to the long axis of the spine, and all exhibit additional faces over and above the normal  $\{104\}$  habit (Fig. 2B). Fig. 2C shows an example of an individual crystal grown epitaxially on the spine surface. It clearly develops one additional specific set of faces, other than the  $\{104\}$ . Other crystallographic directions are unaffected. Synthetic calcite crystals grown de novo from solution in the presence of intracrystalline spine proteins have a similar habit (Fig. 2D). The average angles between newly formed faces and the  $c$ -axis in the overgrown and synthetic crystals are  $15^\circ \pm 2^\circ$  and  $17^\circ \pm 3^\circ$ , respectively. The expressed faces are therefore indexed as the  $\{01l\}$  set ( $l = 1-1.5$ ).

In order to investigate the generality of the observed effect, we also studied skeletal elements from a brittle star. These animals belong to the same phylum (*Echinodermata*) as the sea urchin, and are therefore expected to display similar features. The brittle star skeleton, however, is composed of a variety of morphologically and structurally different skeletal elements, that may provide additional information on localized protein–crystal interactions. Fig. 3A shows one of the plate-shaped skeletal ossicles of a brittle star arm, a tentacle scale. The whole element is a single crystal and the  $c$ - and  $a$ -axes lie in the

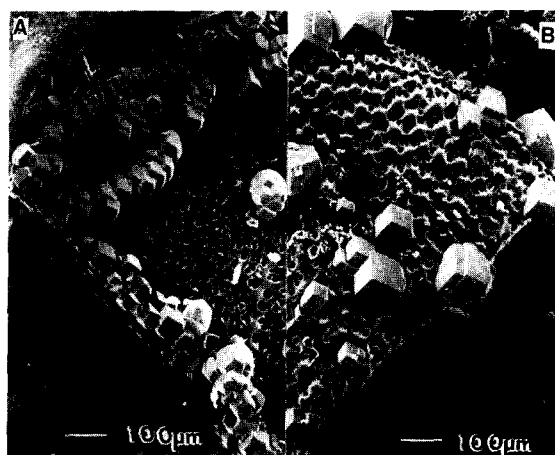


Fig. 4. The inner (A) and outer (B) surfaces of the overgrown dorsal arm plate of the brittle star *Ophiocoma wendti*. Note the differences in the morphology of the overgrown crystals on the two sides of the same element, as well as the differences with those in Fig. 3B.

plane of the ossicle, as can be seen from the uniform orientation of the overgrown crystals (Fig. 3B). The latter express large well-developed  $\{01l\}$  faces (Fig. 3B). In contrast to the tentacle scale, the  $c$ -axis of the dorsal arm plate is perpendicular to the plane of the element (Fig. 4). The crystals overgrown on this ossicle also have additional  $\{01l\}$  faces, but these are systematically less developed than those observed on the overgrown tentacle scale. Furthermore, crystals formed on the

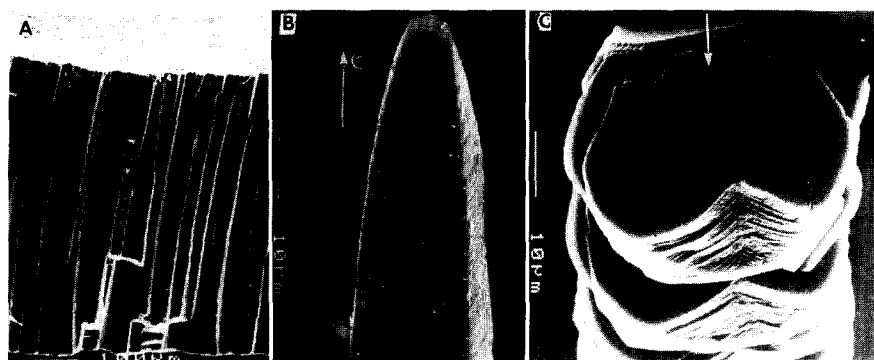


Fig. 5. (A) Fracture surface of the prismatic layer of the mollusc shell *Atrina serrata*. The single crystal prismatic elements are elongated in the direction of the  $c$ -axis. (B) Detail of a single prism isolated from the multicrystalline array in (A). The direction of the  $c$ -axis of the single crystal is indicated. (C) Crystals overgrown on a broken prismatic element. Note the development of the faces perpendicular (indicated by the arrow) and parallel to the  $c$ -axis. The smooth faces are  $\{104\}$ .

edges of the dorsal arm plate, that are roughly parallel to the *c*-axis, express more pronounced {011} faces compared to those on the interior surfaces. Crystals grown on the edges of the tentacle scale, that are perpendicular to the *c*-axis, display the opposite features. We also noted that overgrown crystals are usually much more affected when formed on the inner surfaces of the skeletal elements as compared to their outer surfaces (Figs. 4A and 4B). Thus, the extent to which the overgrown crystals express new faces depends on the morphology and crystallographic orientation of the skeletal element and varies systematically along the substrate.

The morphological modification data of calcitic mollusc prisms [8] suggest two different modes of specific protein intercalation. If so, we would predict an expression of two families of faces in the overgrowth experiment. Fig. 5A shows the fracture surface of the *Atrina* prismatic layer. Each prism (Fig. 5B) is a single calcite crystal, with the crystallographic *c*-axis coinciding with the long axis of the prism. Fig. 5C shows unequivocally that calcite crystals overgrown on the isolated broken prisms do exhibit new faces. They are strongly affected in the *a* and *b* directions, and also express a distinctive rough {001} face.

#### 4. Discussion

We show that epitaxial overgrowth of calcite crystals on biogenic skeletal elements from different phyla (*Echinodermata*, *Mollusca* and *Porifera*) can provide information not only on the orientation of the crystallographic axes within the element, but also on the interactions between the proteins occluded inside the element and the overgrown calcite crystals. This effect was detected by the expression of new families of crystal faces in calcite crystals overgrown on triradiate sponge spicules, and was subsequently confirmed in sea urchin spines, brittle star ossicles and mollusc shell prisms.

The mechanism of expression of the new crystal faces must involve release of proteins into the microenvironment of the skeletal element, due to local dissolution of the crystal surface. The re-

leased proteins are immediately readsorbed on the new growing crystals on specific crystallographic planes. They decrease the crystal growth rates in defined directions, that are consequently expressed as stable crystal faces. The morphological changes correspond to those observed in calcite crystals grown de novo from a solution containing the same specific proteins, thus confirming that these are responsible for the effect.

Crystallization and dissolution, which take place in the same microenvironment, might be due to the presence of magnesium and other ions occluded in the biogenic elements, that are known to increase their solubility relative to the newly grown crystals [15]. Alternatively, the lower thermodynamic stability of biogenic calcite may be accounted for by greater crystal imperfections at the textural level, which in part must be due to the presence of occluded proteins. The former explanation might apply to *Clathrina* sponge spicules, which contain a high percentage of magnesium (16.2 mol%  $\text{MgCO}_3$ ). It is unlikely to apply to *Atrina* shell prisms, which have very small amounts of magnesium (1.5 mol%  $\text{MgCO}_3$ ). As the effect is manifested in a similar fashion in both element types and is even more pronounced in calcitic prisms that have higher concentrations of occluded proteins, the latter explanation may well apply.

The main advantages of this overgrowth technique are that it is relatively simple to perform, requires very small amounts of biogenic material (even tiny skeletal elements can be studied), and it allows identification of protein–crystal interactions under conditions which minimally affect the macromolecules. Although the proteins are not in a “native” state, the observations performed in situ under these conditions are certainly more conducive to preserving macromolecular structure than after isolation and separation procedures, which often result in protein denaturation. The disadvantage of the technique is that all components, i.e. ions and macromolecules, are released together into the microenvironment of the overgrowing crystals, with no possibility of quantifying or separating the effects. The diffusion of released ions is, however, much faster than that of macromolecules. Moreover, the newly

formed {011} faces do not express {011} steps typical for the magnesium affected crystals [8]. Their texture resembles that of the protein affected synthetic crystals. Thus, the major effect, as observed, appears to be due to the released macromolecules.

The new observations derived from these studies are that in various skeletal elements, with different intracrystalline proteins, calcite crystal growth is affected in specific and distinct directions. The sponge spicules and mollusc prisms have occluded proteins, some of which interact with growing crystals along the *c* direction. In contrast, the sea urchin and brittle star elements are only affected in an envelope of six symmetry related planes around the *c*-axis. The information derived from overgrowth experiments is complementary to that observed by other techniques. We note in particular the case of mollusc prisms, where the measured anisotropy in crystal texture is consistent with protein adsorption on the {001} planes [9]. Subsequent overgrowth experiments showed directly the development of the {001} face. However, growth of synthetic crystals in the presence of the total extract of intracrystalline mollusc proteins resulted in non-specifically affected crystals [6]. The overgrown crystals, on the other hand, specifically express both classes of faces, parallel to and perpendicular to the *c*-axis. This confirms that two types of proteins coexist within the biogenic crystals, each able to interact in a specific manner with calcite crystals [8].

We also noted that the extents of nucleation and expression of the new crystal faces on the overgrowth crystals are different in the same element, depending on the location of the crystals and on the orientations relative to the crystallographic axes. For example, extents of nucleation on the outer and inner surfaces of brittle star arm plates differ drastically, as do crystal sizes and the degrees to which these crystals develop specific faces. Furthermore, the crystals overgrown on the dorsal arm plate, a fan-shaped ossicle growing roughly in the *ab* plane of calcite, are much less affected by released proteins than those overgrown on the tentacle scale, a flat element developing roughly in the *ac* plane. One possibility is that different amounts of proteins are occluded

at different sites within the same element, or within various elements of the same organism. An alternative explanation is that the distribution of occluded proteins is more or less the same, but protein release from any surface other than the plane of intercalation is hampered. This factor would cause differences in protein availability in various directions, depending on their orientation relative to the surface of the crystal. The latter interpretation is supported by the comparisons between crystals overgrown on the edges of the brittle star ossicles versus those on the interior surface, and by the observation that crystals formed on the broken ends of mollusc shell prisms, which are roughly parallel to the {001} plane, express much more developed {001} faces than those overgrown on the original pointed end. The presence of proteins, therefore, anisotropically influences the rate of crystal dissolution, in analogy to growth. We conclude that the overgrowth technique can be used to map protein distribution and availability within skeletal elements, as well as provide information on protein–crystal anisotropic interactions *in vivo*.

Function is naturally the most important issue in the study of proteins related to biomineralization, but is poorly understood. Although we are still far from being able to attribute definite functions to intracrystalline proteins, the evidence derived from the overgrowth method, together with that from other techniques, indicates that these proteins are implicated not only in the control of crystal texture and, therefore, mechanical properties, but also in the control of the macroscopic skeletal element morphology [16]. This is particularly evident from a comparison between echinoderm spines and triradiate sponge spicules. The spines are elongated in the *c*-axis direction, and hence growth is reduced in the *a* directions, as the proteins interact preferentially with planes more or less parallel to the *c*-axis. The spicule rays develop in the *ab* plane, and consistently the proteins interact specifically on the planes perpendicular to the *c*-axis. Similar observations have been made on several other calcitic sponge spicules (in preparation). The fascinating possibility exists, therefore, that skeletal element morphology is controlled not only by the

shape of the preformed space in which the crystal grows, but also by the assemblage of proteins introduced into the crystal growing solution.

### Acknowledgments

We thank Dr. Micha Ilan (Tel-Aviv University, Israel) for his most helpful advice and for providing us with the sponge specimens. We also thank Dr. Gordon Hendler (Natural History Museum of Los Angeles County, California) for the brittle stars, and Professor Scott Brande (University of Alabama, Birmingham) for the bivalve specimens. S.W. is the incumbent of the I.W. Abel Professorial Chair of Structural Biology and L.A. is the incumbent of the Patrick A. Sherman Professorial Chair of Biological Ultrastructure. This study was supported by a grant from the US–Israel Binational Science Foundation.

### References

- [1] K. Simkiss and K.M. Wilbur, *Biom mineralization; Cell Biology and Mineral Deposition* (Academic Press, San Diego, CA, 1989).
- [2] H.A. Lowenstam and S. Weiner, *On Biomineralization* (Oxford Univ. Press, Oxford, 1989).
- [3] A. Veis, in: *Biom mineralization; Chemical and Biochemical Perspectives*, Eds. S. Mann, J. Webb and R.J.P. Williams (VCH, Weinheim, 1989) pp. 189–222.
- [4] A.P. Wheeler and C.S. Sikes, in: *Biom mineralization; Chemical and Biochemical Perspectives*, Eds. S. Mann, J. Webb and R.J.P. Williams (VCH, Weinheim, 1989) pp. 95–132.
- [5] S. Mann, in: *Biom mineralization; Chemical and Biochemical Perspectives*, Eds. S. Mann, J. Webb and R.J.P. Williams (VCH, Weinheim, 1989) pp. 35–62.
- [6] A. Berman, L. Addadi and S. Weiner, *Nature* 331 (1988) 546.
- [7] I. Weissbuch, L. Addadi, M. Lahav and L. Leiserowitz, *Science* 253 (1991) 637.
- [8] S. Albeck, J. Aizenberg, L. Addadi and S. Weiner, *J. Am. Chem. Soc.* 115 (1993) 11691.
- [9] A. Berman, J. Hanson, L. Leiserowitz, T.F. Koetzle, S. Weiner and L. Addadi, *Science* 259 (1993) 776.
- [10] W.C. Jones, *Quart. J. Microsc. Sci.* 96, Part 2 (1955) 129.
- [11] K.M. Towe, W.-U. Berthold and D.E. Appleman, *J. Foraminiferal Res.* 7 (1977) 58.
- [12] K. Okazaki, R.M. Dillaman and K.M. Wilbur, *Biol. Bull.* 161 (1981) 402.
- [13] E.A. Minchin, *Quart. J. Microsc. Sci.* 40 (1898) 469.
- [14] W.J. Schmidt, *Zool. Jahrb. Allgem. Zool.* 47 (1930) 357.
- [15] F. Lippman, *Sedimentary Carbonate Minerals* (Springer, Berlin, 1973).
- [16] L. Addadi, J. Aizenberg, S. Albeck, A. Berman, L. Leiserowitz and S. Weiner, *Molecular Crystals and Liquid Crystals Sci. Technol.*, in press.